

Lab on chip device for separation of Plasma from Blood

R.Aishwarya

A Dissertation Submitted to
Indian Institute of Technology Hyderabad
In Partial Fulfillment of the Requirements for
The Degree of Master of Technology



भारतीय प्रौद्योगिकी संस्थान हैदराबाद
Indian Institute of Technology Hyderabad

Department of Electrical Engineering

June, 2016

Declaration

I declare that this written submission represents my ideas in my own words, and where others' ideas or words have been included, I have adequately cited and referenced the original sources. I also declare that I have adhered to all principles of academic honesty and integrity and have not misrepresented or fabricated or falsified any idea/data/fact/source in my submission. I understand that any violation of the above will be a cause for disciplinary action by the Institute and can also evoke penal action from the sources that have thus not been properly cited, or from whom proper permission has not been taken when needed.

R. Aishwarya

R.Aishwarya

EE13M1027

Approval Sheet

This thesis entitled **Lab On Chip for Separation of Plasma from Blood** by R.Aishwarya is approved for the degree of Masters from IIT Hyderabad

Smishir Kumar

SMISHIR KUMAR
EE, IITH.

Examiner

✓

Examiner

Shiv Govind Singh

Dr. Shiv Govind Singh
Associate professor, Dept. of EE,
IIT Hyderabad

Advisor

Dr. Kaushik Nayale

Dr. Kaushik Nayale
EE, IIT Hyderabad.
Chairman

Acknowledgements

First of all I want to acknowledge Dr. Shiv Govind Singh sir for his consistent guidance, support and help. All the transparent discussions and philosophies were very helpful to me.

I am willing to thank Dr. Siva Rama Krishna sir and Dr. Asudeb Dutta sir for helping me with their research experience. I am also grateful to Satish Bonam and Jose for helping me through out in my project.

Dedicated to

My Family and friends.....

Abstract

Microfluidics has developed as a set of powerful tools that have greatly advanced in some areas of biological research. The use of microfluidics has enabled many experiments that are otherwise impossible with conventional methods and is highly capable of providing advantages in terms of a significant reduction in the sample processing time, sample volumes, and consumption of costly reagents. Various research groups have established continuous flow separation methods in microfluidic devices; however, they have worked with relatively small dimension microchannels (similar to the blood cell diameter). The present work demonstrates separation of plasma by utilizing the hydrodynamic separation techniques in microchannels with size of the order of mm. The separation process exploits the phenomenon, which is very similar to that of plasma skimming explained under Zweifach-Fung bifurcation law. The T microchannel device (comprising perpendicularly connected blood and plasma channels) were micro-fabricated using su8 negative photo resist and for calculating the efficiency of the device electrodes were deposited on both the substrates. Three variables (feed hematocrit, main channel width, and flow rate distributions) were identified as the important parameters which define the device's efficiency for the blood plasma separation.

Contents

Declaration.....	ii
Approval Sheet	iii
Acknowledgements.....	iv
Abstract.....	vi
Chapter 1 Introduction	1
Chapter 2 Literature Survey.....	7
Chapter 3 Fabrication results.....	16
Chapter 4 Experiment and characterization	29
Chapter 5 Conclusion and Future Work.....	40
References.....	

Chapter 1

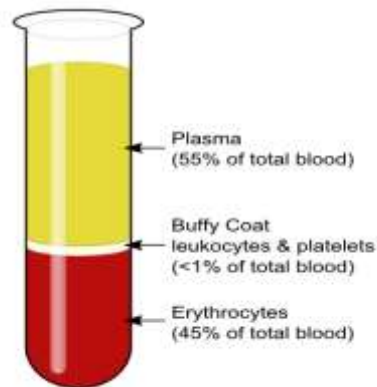
Introduction

The separation of plasma from blood is an indispensable process in the domain of disease diagnostics. Human blood plasma provides crucial information pertaining to disease diagnostics as innumerable biomarkers are found in blood plasma, which state the physiological state of the human body. Therefore, the plasma separation from whole blood is necessary for disease diagnostics.

The conventional method of plasma separation (centrifugation), though commonly employed, is rather laborious and time consuming, and cannot be integrated with a biosensor to develop a point-of-care micro device. The field of microfluidics has shown tremendous potential to provide distinct insights and improvised solutions to processes hitherto involving complex traditional experimental methods, especially in the areas of biology and clinical diagnostics. The excitement surrounding microfluidics rests on the fact that it is highly capable of providing advantages in terms of a significant reduction in the sample processing time, sample volumes, and consumption of costly reagents, as well as precision in controlling fluid assays, among others.

1.1 Centrifugation:

Centrifugation, Plasma separation is achieved by subjecting the suspension to natural or induced gravitational fields. Blood cells are denser than the liquid medium of plasma. These cells would settle down due to gravitational forces and form a zone with a very high blood cell density. This method is worth nothing that the method is used for separating different blood cells.



This is the conventional method and the commonly used method for separating plasma, requires considerable amount of time and effort, and which cannot be integrated with a biosensor to develop a point-of-care device.

1.2 Microfluidics:

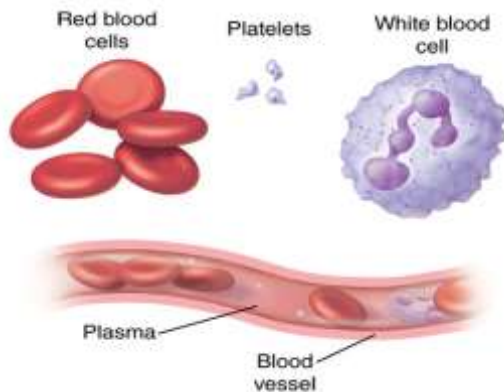
Microfluidics has developed as a set of powerful tools that have greatly advanced in some areas of biological research. The use of microfluidics has enabled many experiments that are otherwise impossible with conventional methods and is highly capable of providing advantages in terms of a significant reduction in the sample processing time, sample volumes, and consumption of costly reagents.

1.3 Blood:

Blood is a multiphase fluid, composed of cells suspended in plasma. The main components of blood are erythrocytes (red blood cells), leukocytes (white blood cells), thrombocytes (platelets) and plasma.

Blood mainly comprises about 45%–50% red blood cells, ~1% of white blood cells and platelets, and the remaining ~55% is a pale or straw yellow colored fluid called plasma. Human blood plasma contains 91% water, 7% proteins, 2% inorganic ions, and other organic substances.

Blood exhibits a complex behavior even at a very high concentration of cells and behaves as a fluid. Whole blood is a non-Newtonian fluid, whereas plasma is a Newtonian fluid



1.4 Definitions:

1. Hemolysis:

The breakage or the destruction of a cell membrane, especially RBCs, thereby releasing its contents, such as hemoglobin, into the surrounding plasma or additive solutions.

2. Hematocrit:

The hematocrit (Hct) or packed cell volume (PCV) or erythrocyte volume fraction is the proportion of blood volume that is occupied by red blood cells. Its normal range is 0.47 ± 0.07 in adult males and 0.42 ± 0.05 in adult females. PCV can be determined by centrifuging blood.

3. Serum:

Serum is similar to plasma in composition, but without fibrinogen (clotting factor), and is obtained on centrifugation of blood without prior addition of anticoagulant.

4. RBC aggregation:

The human blood tends to form reversible aggregates, sometimes referred to as ‘rouleaux’ formation. RBC aggregation is promoted by fibrinogen or plasma proteins.

5. Plasma skimming:

The depletion of blood cells near the channel walls. It is utilized to withdraw plasma into a side branch.

6. Separation efficiency:

Also referred to as purity. It is the measure of the number of RBCs in the collected plasma against the RBC count in the inlet blood sample. There is no universal agreement on the definition among researchers, and the separation efficiency values obtained differ based on the definition employed. Generally, it is defined as

$$\eta = \frac{c_s - c_p}{c_s} * 100$$

- , where η is the separation efficiency
- c_s = Number of cells per μl in source/feed blood at inlet of microchannel
- c_p = Number of cells per μl in depleted cell branch or plasma collection outlet of the microchannel

Separation efficiency of 100% refers to the situation in which no cells are detected in the collected plasma sample.

6. Yield:

Also referred to as extraction rate. This is the ratio of flow rate at the outlet plasma collection zone to the flow rate of the inlet blood sample. For example, a 3% yield can be interpreted as obtaining 30 μL plasma from 1 ml of blood.

7. Flow rate ratio:

Given a bifurcation in the microchannel with varying flow rates, the ratio of the higher flow rate to the lower flow rate is defined as the flow rate ratio, if not specifically defined otherwise.

$$F_Q = \frac{Q_1}{Q_2} = \frac{L_p W_b \left\{ 1 - 0.63 \left(\frac{h_b}{W_b} \right) \right\}}{L_b W_p \left\{ 1 - 0.63 \left(\frac{h_p}{W_p} \right) \right\}}$$

- L_p and W_p are the length and width of plasma channel, respectively;
- L_b and W_b are the corresponding dimensions for the main blood channel.

8. Poiseuille's law:

For a Newtonian, incompressible fluid exhibiting laminar flow in cylindrical tubes where is pressure drop per unit length, Q is the flow rate, D is the tube diameter, μ is dynamic viscosity.

9. Reynolds number (Re):

The ratio of inertia force and viscous force, formulated as

$$Re = \frac{\rho v d_h}{\mu}$$

- $d_h = \frac{4 \cdot \text{Area of microchannel}}{\text{Perimeter of microchannel}}$
- $v = \frac{\text{Total Flow rate}}{\text{area of the microchannel}}$
- d_h is the hydraulic diameter
- v is the average velocity
- ρ = density of blood
- μ = viscosity of blood.

10. Dean drag:

In the presence of secondary flow in curved channels due to centrifugal and inertial forces, the magnitude of secondary flows can be described by the Dean number, defined as $De = Re d R h$, where Re is the Reynolds number, d_h is the hydraulic diameter of the channel, and R is the radius of the curvature.

11. Bifurcation law:

It states that: when RBCs flow through a bifurcation region of a capillary blood vessel, they have a propensity to move into the daughter vessel, which has the higher flow rate, leaving a relatively small number of cells in the lower flow rate vessel.

1.5 Thesis outline: The thesis is arranged as follows: Section 2 explores some possible physical reason behind the separation phenomenon in larger dimension T-microchannel, employed in the present work.. Details about process flow and fabrication are presented in Sections 3 followed by conclusions in Section 6.

Chapter 2

LITERATURE SURVEY

2.1 Microfluidic methods:

Microfluidic methods for blood plasma separation include both passive separation and active separation methods. In non-inertial or active methods, separation is achieved by the application of external force fields such as electrical and magnetic fields. However, to achieve separation, passive methods rely on effective microchannel design, inertial effects, flow rate control, and utilize multiple biophysical effects such as the Fahraeus effect and the Zweifach-Fung bifurcation law.

2.1.1 The active separation methods:

In non-inertial or active methods, separation is achieved by the application of external force fields such as electrical and magnetic fields. Active systems generally use external fields (e.g., acoustic, electric, magnetic, and optical) to impose forces to displace cells for sorting, whereas passive systems use inertial forces, filters, and adhesion mechanisms to purify cell populations. Cell sorting on microchips provides numerous advantages over conventional methods by reducing the size of necessary equipment, eliminating potentially biohazardous aerosols, and simplifying the complex protocols commonly associated with cell sorting.

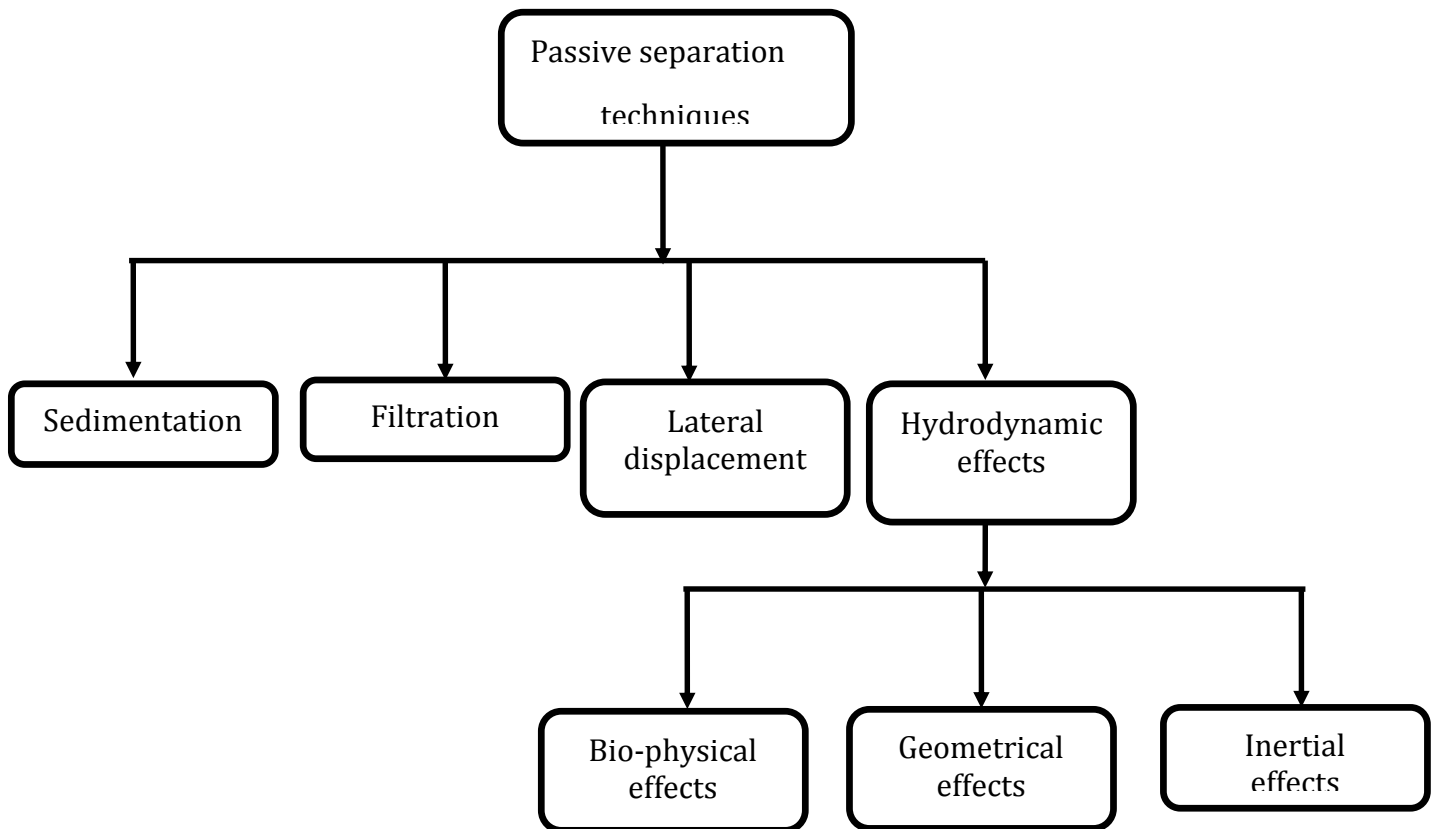
2.1.2 The passive separation methods:

Passive separation methods are mostly preferred because these methods do not require application of an external force field, thereby allow for efficient system integration. Success in the passive method pertains to intelligently manipulating the

microchannel pathways such that during blood flow, RBCs skim-off from whole sample blood.

The advantages of passive separation methods are their simplicity of design, ease of fabrication, continuous operation, use of moderate to high flow rates, and ease of integration with a biosensor.

Microdevices based on passive separation methods for blood plasma separation are further classified as lateral displacement by obstacles, sedimentation, filtration, and hydrodynamic effects.



The efficiency of these microfluidic devices is judged in terms of purity that is the quantity of plasma obtained, and the total time taken for the separation. In fact, the biggest challenge lies in separating plasma without diluting the blood, and also subjecting the cells to minimal stresses during the separation process.

A high stress level leads to RBC lysis or hemolysis that liberates free hemoglobin, which interferes with the diagnosis of the required biochemical in blood. This will make it difficult for effective treatment and medication to the patient. Therefore care has to be taken in designing such a microdevice for blood plasma separation to ensure that the sample obtained would be free from hemolysis to the greatest extent possible.

The final goal of a good microfluidic device in such an application would involve extraction of high quality plasma, in the minimum possible time, and without losing any target analytes.

2.2. The RBCs:

A few researchers have shown that, depending upon the diameter of the vessel in which blood flows, it behaves either as a single phase homogeneous fluid or a multi-phase, nonhomogeneous fluid.

In vessels of large diameters, blood can be thought of as homogeneous and treated as a single-phase fluid, and analysis can be carried out satisfactorily based on this assumption. In vessels with a smaller diameter, blood begins to exhibit multi-phase, non-homogeneous and non-Newtonian characteristics, resulting in the appearance of apparent viscosity; this is mainly due to the deformable nature of the RBCs.

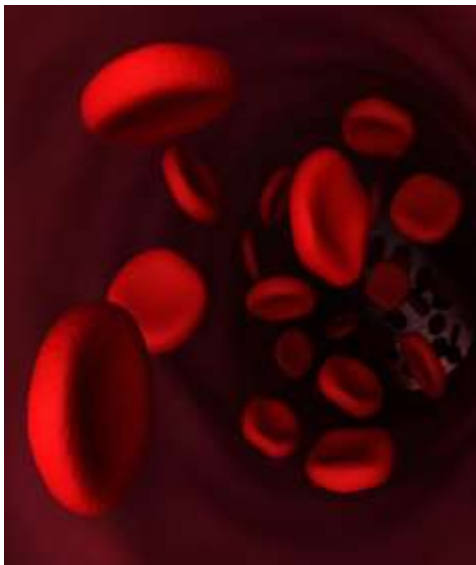
Blood without the presence of cells i.e. plasma can be considered as a Newtonian fluid. The non-Newtonian behavior of blood is attributed to the presence of cellular components

The uniqueness of RBC structure is its elasticity and deformability. In a healthy adult, the average size of an RBC is approximately $8\ \mu\text{m}$ with a thickness of about $2\ \mu\text{m}$.

The deformable nature of RBCs allows cells to flow through narrow vessels which are much smaller than the size of the RBC. The axial migration of cells away from the walls is increasingly manifested with a decrease in vessel diameter; this phenomenon is also prompted by the deformability of cells. The outcome of the axial

migration is a cell-free layer adjacent to the walls, and has led to observations of many biophysical effects.

The deformable nature of RBCs is a boon for the sustenance of life, but it poses a challenge to the plasma separation designer to formulate a mathematical model describing cell mechanics. The RBCs carry hemoglobin, but when the cells are subjected to very high stresses, there is a very high chance of RBC rupture leading to hemolysis. The occurrence of hemolysis can be identified by the discoloration of the plasma.



Another interesting phenomenon observed in blood is the reversible aggregate formation of RBCs, which is owing to the presence of fibrinogen and plasma protein. The aggregates' size is inversely proportional to the magnitude of shear forces that the blood is subjected to.

2.3 Theoretical background:

2.3.1. Biophysical effects

CFL:

In microcirculation, RBCs have a tendency to migrate towards the axis of the tube, thereby increasing the cell concentration along the center while leaving a marginal zone devoid of cells along the channel walls, called the cell-free layer (CFL).

Deformability of the cells is attributed as one of the reasons for the axial migration of cells; high shear zones near the wall are also responsible for the axial migration of the cells. This in turn increases the velocity of the RBCs compared to that of plasma.

The cell-free layer thickness is dependent on the cell concentration, deformability, vessel diameter, cell aggregation, and flow rate. The thickness of the CFL decreases with an increase in tube diameter and with an increase in hematocrit level. When cell concentration (hematocrit) is high, the crowding effect acts against axial migration, resulting in a decrease in the cell-free layer. An increment in flow rate also has a positive effect on the thickness of the CFL at the microchannel periphery.

Another important phenomenon in microcirculation is phase separation at single bifurcations. This phenomenon has been the subject of ongoing research. Feed hematocrit, channel width, and flow rate distribution have been elucidated as important parameters influencing the phase separation.

Svanes and Zweifach observed that when the parent vessel of a bifurcation had a high velocity, the vessel hematocrit in the side branch could be reduced to almost zero by decreasing the blood flow through the branch.

Subsequently, several studies have been carried out reporting the disproportionate distribution of RBCs at a bifurcation. Fenton studied Parameters which influence the disproportionate cell distribution at the bifurcation. Three parameters of major importance were identified as feed hematocrit, tube diameter and flow rate ratio.

Given different flow rates of the two daughter channels in the capillary bifurcation, the cell, on reaching the bifurcation, faces a dilemma about choosing the channel flow to follow. Cells tend to prefer the channel with the higher flow rate in comparison to the channel with the lower flow rate (figure 2).

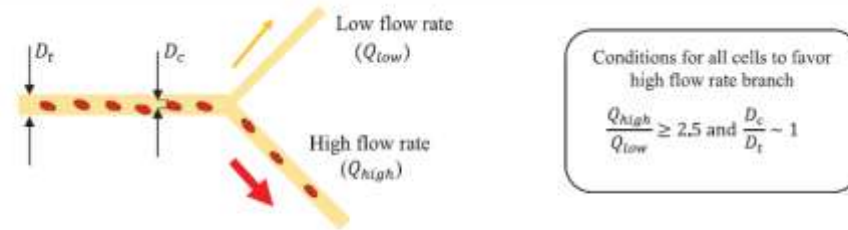


Figure 2. Schematic of the Zweifach–Fung bifurcation law. D_c and D_t represent the diameter of the cell and channel (tube) respectively.

For this asymmetric and preferential distribution of cells to occur, the velocity ratio of the daughter channels is to be of the order 2.5:1, provided that the channel diameter to cell diameter ratio is of order one. The exact critical velocity ratio is dependent upon many competing factors, but essentially is a function of the cell to tube diameter ratio and elasticity, and deformability of the blood cells. This is called the Zweifach–Fung bifurcation effect, and is schematically represented in figure 2. It can be observed that a cell, on reaching the zone of bifurcation, tends to favor the channel with the higher flow rate, thereby leaving the channel with a low flow rate with relatively fewer or no cells at all.

In general, it has been shown that the cell, on reaching the zone of bifurcation, experiences an asymmetric pressure and shear distribution, with their resultant towards the direction of the channel with higher flow rate. This asymmetric pressure and shear on the blood cells is due to a non-uniform (parabolic distorted) velocity profile, as noted in section 2. Lately, some researchers have pointed out that the cell-free region along the channel walls has a role to play in this distribution of cells at the bifurcation

In general, to understand the biophysical effects, most of the experimental studies have been performed on tubes with a circular cross section. However, most of the microfluidic devices which are fabricated today are noncircular (trapezoidal, square, rectangular, triangular) in cross section.

Therefore, some confusion exists in the literature about the validity of the bifurcation law or other biophysical effects with respect to noncircular cross sections

Roberts and Olbricht studied the behavior of spherical particles suspended in a fluid flowing in a microchannel with a rectangular cross section. They showed that

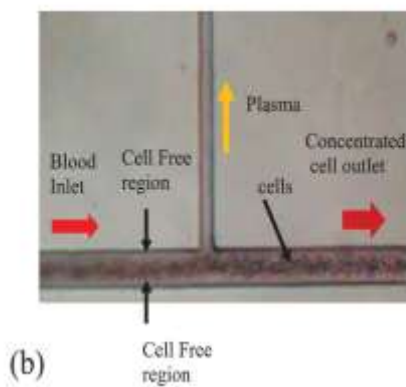
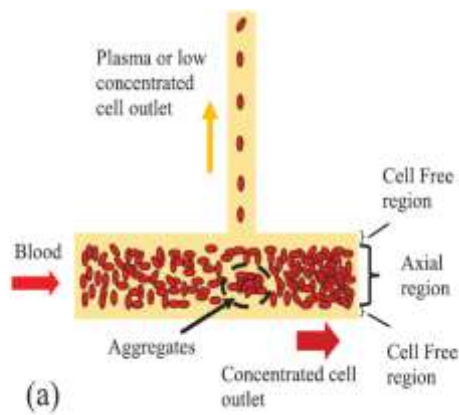
there is still an asymmetric distribution of the particles in the daughter channels of the bifurcation. Also, they studied the influence of the aspect ratio on separation and concluded from their findings that at low Reynolds number, it is the aspect ratio of the cross section which plays a significant role in particle partitioning instead of the absolute dimensions of the channels.

The channels fabricated with materials other than glass, such as PDMS (polydimethylsiloxane). One such study is by Lima *et al*, who studied blood flow behavior in a rectangular PDMS microchannel. They considered blood flow (~20% Hct diluted with physiological saline) in a $300\ \mu\text{m} \times 45\ \mu\text{m}$ rectangular channel for Reynolds number up to 0.1 and found that the cells do not axially migrate towards the center axis. However, on reducing the microchannel width to $100\ \mu\text{m}$, they found a thin plasma layer free from cells near the wall of the microchannel. Their study suggests that blood flow and the related biophysical effects, such as the Fahraeus effect, are observed even in PDMS channels, but the results obtained may be slightly different from those of glass based microchannels

2.3.2. Combination of biophysical and geometrical effects:

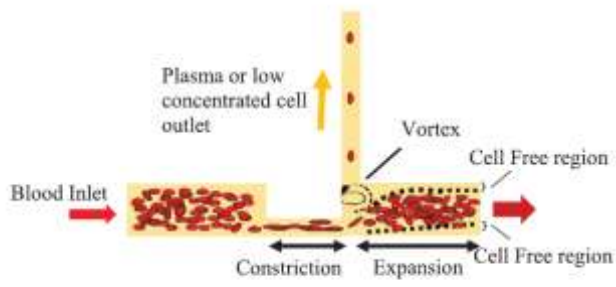
Examples:

As blood flows through the microchannel, the axial migration of the cells is clearly visible, thereby leaving a clear cell-free region adjacent to the walls.

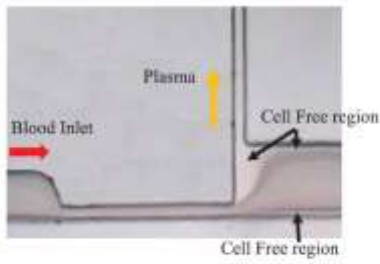


Due to axial migration, the cells have higher velocity relative to the adjacent plasma in the cell-free layer. Additionally, the cells are of higher density in comparison to plasma. Therefore, the momentum of cells is higher compared to plasma, which results in an enhancement of the cell-free layer immediately after the expansion. The cell-free region thickness may depend on hematocrit, flow rate, dimensions of the constricted channel, and deformability of cells

It is clearly observed that by employing constriction-expansion in the design, there is a definite increase in the cell-free region at the zone of expansion. However, increasing the constriction ratio or flow ratio beyond a critical value is counterproductive as the corner vortices at the zone of the expansion become so strong that they tend to drag the particles from the blood outlet channel into the plasma channel.



(a)



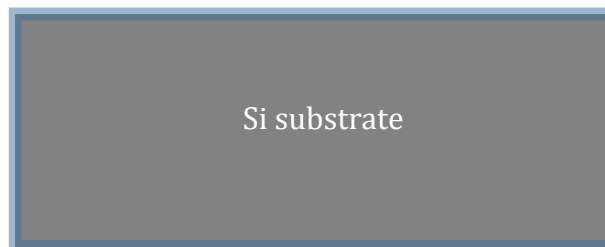
(b)

Chapter 3

PROCESS FLOW AND FABRICATION RESULTS

3.1 Process flow:

Choosing substrate substrates: silicon as 1st substrate and a glass substrate as 2nd wafer.



Step 1:

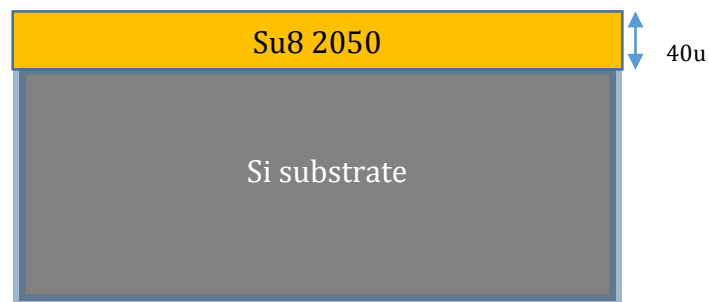
Silicon Wafer Clean and Dehydration

A silicon wafer is subjected to a 12 minute basic clean in Piranha solution. Piranha solution is a mixture of sulfuric acid (H_2SO_4) and hydrogen peroxide (H_2O_2). The basic clean was performed at 70 degree C. A five second dip in Buffered Oxide Etch (BOE), containing hydrofluoric acid, was also performed to remove the native oxide. The wafers are then rinsed and dehydrated at 200 °C for 30 minutes to evaporate all solvents from the wafer to prevent improper adhesion of SU-8.

Step 2:

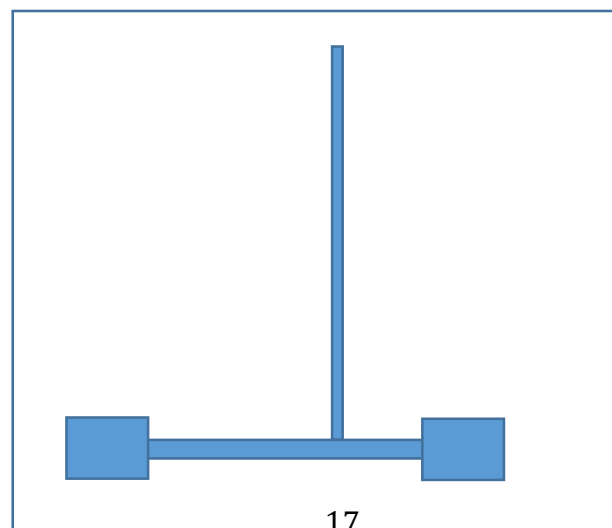
40um T shaped channel formation:

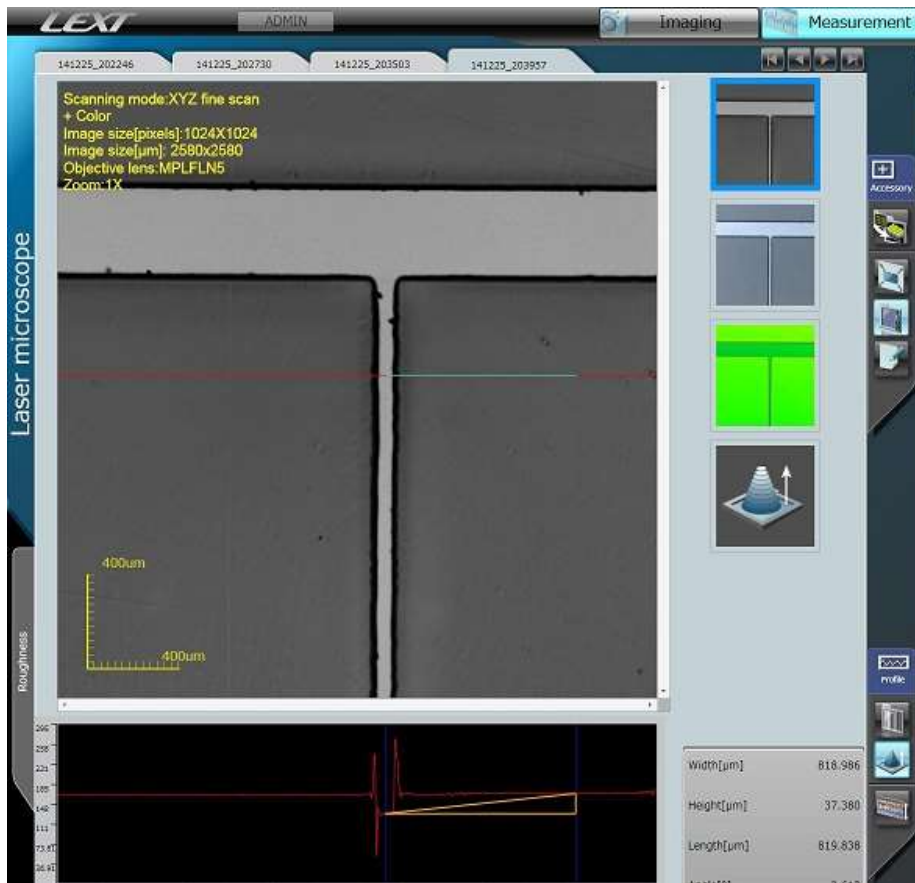
Spin coating was then performed to obtain a uniform SU-8 layer. A spread cycle of 100 rpm at 300 rpm/s was used to distribute the SU-8 2050 across a silicon and a following thickness dependent cycle of 2000 rpm at 300 rpm/s was used to obtain a thickness of 40 μm . After spin coating the wafers were transferred to a hot plate to perform a stepped soft bake. The step includes a transfer from a hot plate of 65 $^{\circ}\text{C}$ for 4 minutes to a 95 $^{\circ}\text{C}$ hot plate for 7 minutes. The soft bake is meant to drive solvents from the polymer film and to dry the film for subsequent handling. The silicon wafer was exposed for 45 sec to form microchannels within the SU-8 layer.



#Mask1

To define main channel, plasma channel and reservoirs.





Step3:

Formation of Ti electrode: Using PPR

Spin coating with a cycle 3000 rpm at 300 rpm/s was used.
The wafer was exposed for 22sec to form opening for electrode deposition.

#Mask2:

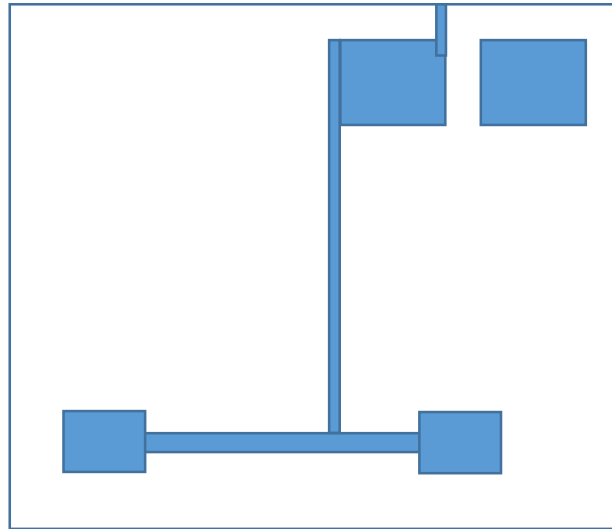


Step 4:

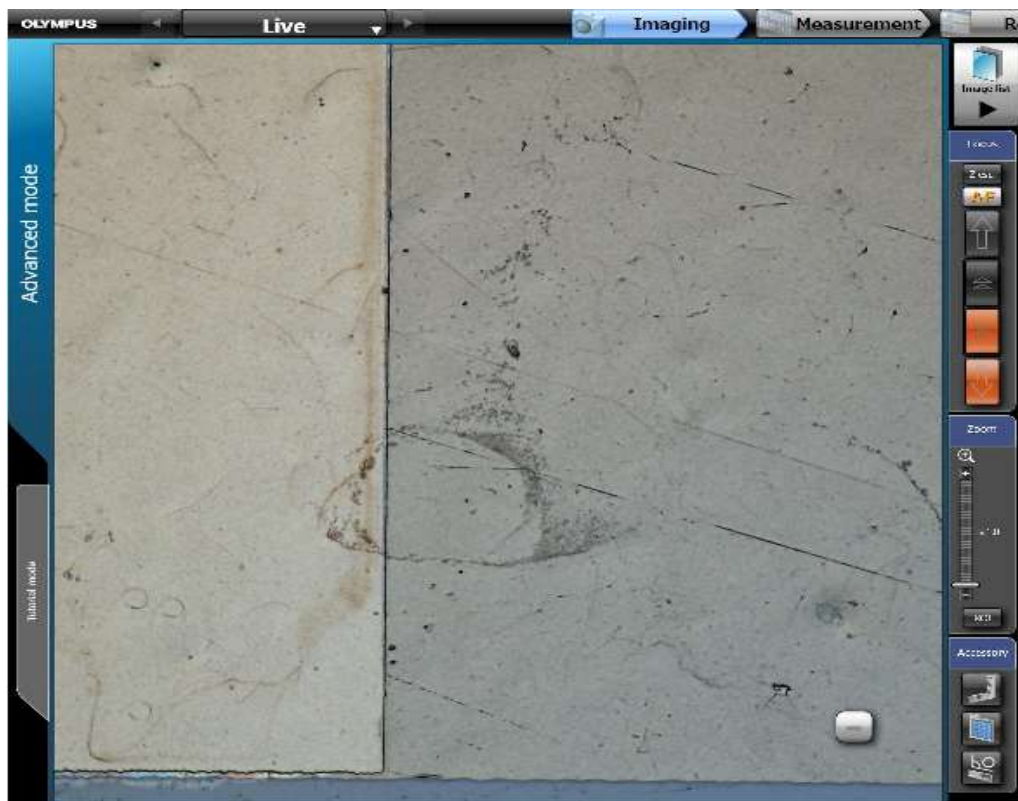
Formation of 10um channel on electrode: Using su8 2010

Spin coating was then performed to obtain a uniform SU-8 layer of 10um all over. A spread cycle of 100 rpm at 300 rpm/s was used to distribute the SU-8 2010 across a silicon and a following thickness dependent cycle of 3000 rpm at 300 rpm/s was used to obtain a thickness of 10 μm . After spin coating the wafers were transferred to a hot plate to perform a stepped soft bake. The step includes a transfer from a hot plate of 65 $^{\circ}\text{C}$ for 1minutes to a 95 $^{\circ}\text{C}$ hot plate for 4 minutes. The silicon wafer was exposed for 33sec to form microchannels within the SU-8 layer.

#MASK3:







Step 5:

To prevent later contamination of the glass wafer, fluid input and output holes were first drilled through the glass substrate. A 1.5 mm drill bit was used to create the holes at spin speed of 3000 RPMs. Constant drips of coolant were applied to cool the bit and wash away debris.

These holes were aligned to be in the same location as the masked region of future metal deposition step. This will eventually create a complete passage through the wafer for fluid input/output attachments.

The glass wafer and a new silicon wafer are then subjected to a 12 minute basic clean in Piranha solution. Piranha solution is a mixture of sulfuric acid (H_2SO_4) and hydrogen peroxide (H_2O_2). The basic clean was performed at 70 degree C. The wafers are then rinsed and dehydrated at 200 degree C for 30 minutes to evaporate all solvents from the wafer to prevent improper adhesion of SU-8.

Step 6:

Formation of Ti electrode on 2nd wafer:

Using hard mask



Step 6: Bonding:

Bonding silicon substrate to glass substrate.

BONDING PROCEDURES:

1. PDMS BONDING:

Mixing the PDMS

PDMS should be mixed in a 1:10 ratio of curing agent and PDMS monomers. The PDMS monomers are much more viscous than the curing agents. Stir the mixture for approximately 3 minutes. After the 3 minutes of stirring the mixture will have many air bubbles. These bubbles must be removed

before the PDMS can be used to make a device. To degas the PDMS, we expose the mixture to a vacuum. The vacuum causes the bubbles in the PDMS mixture to expand and rise to the surface where they pop. To degas the PDMS, we expose the mixture to a vacuum. Do not leave the PDMS in the vacuum for too long because it will become more viscous and will prevent bubbles from rising to the surface when the PDMS is poured into the mould.

Once the PDMS has been degassed. Spin coat this PDMS onto glass substrate at 3500rpm. Now align both the substrates and bond them and heat it at 70°C for an hour.

2. SU8 BONDING:

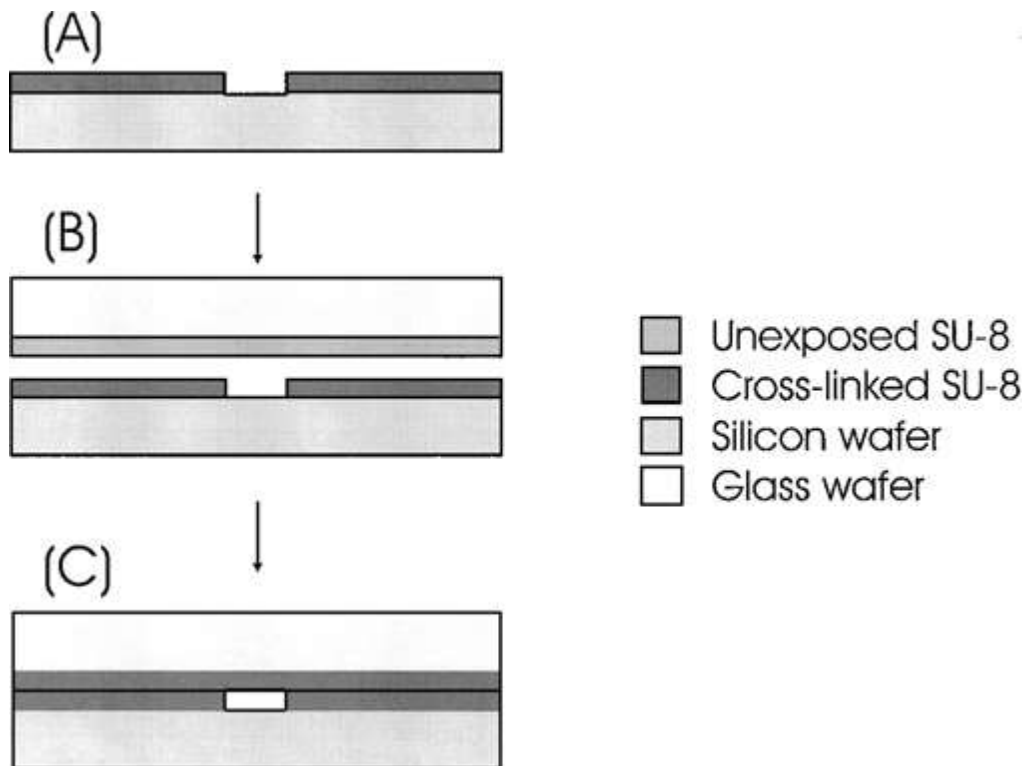
Adhesive bonding has become a major wafer bonding technique in microelectro-mechanical systems (MEMS). In this method polymeric material is used as an adhesive layer between wafers to be bonded. The method has various advantages over more traditional bonding techniques such as anodic bonding or thermo-compression. Temperatures can be lower than 100 °C during adhesive bonding process, enabling wider selection of materials applied on the bonded wafers. Low cost and large selection of wafers to be bonded and large number of polymers to be used for bonding are other advantages of adhesive bonding. This is acceptable in many microfluidic and packaging applications. Material selection for adhesive bonding is large: epoxies, polyimides, fluoropolymers, negative and positive photoresists. SU-8 is epoxy-based negative resist developed by IBM. Today it is widely applied in the field of MEMS because of its unique properties. Compared with traditional MEMS fabrication methods, SU-8 offers a cheap and easy fabrication process to produce high aspect ratio structures.

SU-8 has been used in fabrication of closed channels and cavities. SU-8 closure has been done with different adhesives like PVC or other epoxies. SU-8 itself has also been used in adhesive bonding. Advantage of using SU-8 for bonding is that it creates strong bonds with itself by cross-linking. In some applications like in electrophoretic separation devices it is

preferable to have the whole structure made out of one material only.

Applications of SU-8 as bonding adhesive have been mainly in microfluidic devices

SU-8 served both as a material for the channels and also as a bonding adhesive.



SU-8 layers from 50_μm to 100_μm thickness were applied. Baking times, bonding temperature and exposure of this layer were optimized for the bonding process. Similar to structural layer, also the bonding layer was soft baked on a hot plate followed by contact with structural wafer during cooling. Pressure was applied to initiate contact between wafers. Bonding layer was exposed through the glass wafer and post exposure bake was done to finish bonding by cross-linking of the bonding layer. Unlike reference no additional pressure was applied after initial contact was made. Expensive vacuum bonding system that is often used in adhesive bonding was not required. Bonding process was also investigated for fabrication of fully insulated structures. In this method a blanket SU-8 layer was spun on a

silicon wafer. Blanket exposure of SU-8 was followed by post exposure bake. On top of the first SU-8, second SU-8 layer was spun and patterned as described above. Structures made fully of SU-8 are beneficial not only because of good thermal and electrical isolation but also because of symmetry and mechanical stresses. This is an advantage for example in fabrication of microchannels.

Relatively thick bonding layer (50–100_μm) was applied to compensate thickness irregularities of the structural layer. Bonding close to glass transition temperature of SU-8 allowed slight flow of the bonding layer, enabling sealing of large areas. Bonding at this temperature caused unintentional gap filling and possibly some other deformation of the structures. These parameters have been investigated and discussed in this section. Unless otherwise stated, the discussion below is for 65_μm thick bonding layer.

In optimized bonding procedure for 65_μm bonding layer samples were soft baked on a hot plate keeping temperature at the beginning 15 minutes in 65 °C to planarize the layer. After that temperature was ramped up to 95 °C and kept there for 10 minutes. Glass wafer with adhesive SU-8 was cooled down to 68 °C (ramp rate 3 °/min) and the wafer with SU-8 structures was heated up to 68°, and the wafers were pressed together.

This thermal equalization reduced structure deformation during bonding. At this temperature void formation was minimized and unintentional gap filling was controlled. Bonding temperature of 68 °C is between earlier published results 75 °C and 48 °C .

Pressure to the bonded wafers was applied from one edge and continued over whole wafer. This reduced the amount of air bubbles between bonded layers. Apart from initiation, pressure was not applied during bonding procedure. After contact is achieved over the whole wafer, second layer of SU-8 is exposed through the glass wafer with a dose of 1000mJ/cm². In post exposure bake temperature was first ramped to 95 °C in 5 minutes followed by holding there for 5 more minutes. Again slow cooling was required to reduce stresses in the bonded stack.

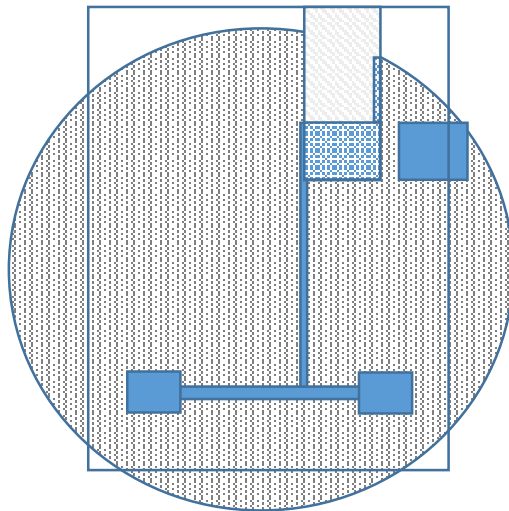
By optimization of processing parameters, reasonably good bonding results were achieved. Temperature during bonding should be adjusted to be close to glass transition of SU-8 to avoid complete filling of the structures. By lowering the

bonding temperature, filling of the structures can be reduced, but bonding quality suffers. At lower temperatures non-bonding area increases. Below 60 °C high pressure was required to achieve contact. Removal of pressure lead to debonding when contact was made below glass transition temperature of SU-8. Bonding also failed if wafer was held at 95 °C for too long time during soft bake. However, bake should be reasonably long because the amount of solvent should be minimized during soft bake, as the remaining solvent reduces cross-linking density and therefore bonding strength.





Final Device looks as follows:

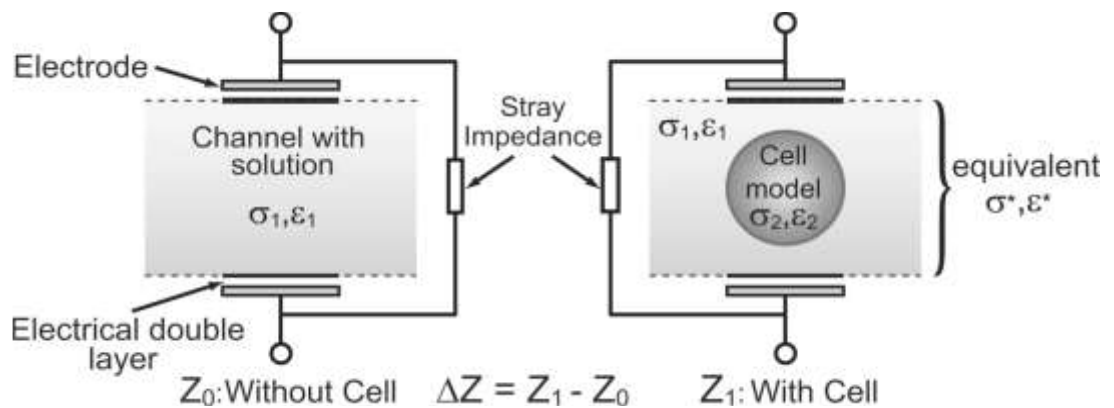


CHAPTER 4

EXPERIMENTAL SETUP & CHARACTERIZATION

The efficiency of these microfluidic devices is judged in terms of purity that is the quantity of plasma obtained, and the total time taken for the separation. In fact, the biggest challenge lies in separating plasma without diluting the blood, and also subjecting the cells to minimal stresses during the separation process. The final goal of a good microfluidic device in such an application would involve extraction of high quality plasma, in the minimum possible time, and without losing any target analytes. The quality plasma is known by counting the cells left in plasma after separation.

Over the last century a number of techniques have been developed which allow the measurement of the dielectric properties of biological particles in fluid suspension. Generally, in these devices, a constant current is set across a small aperture using a pair of large electrodes and a voltage pulse is recorded as each cell passes through the high current density opening. De Blois and Bean used an approximation of the Laplace equation solution to determine, in a cylindrical aperture with an axial electric field, the resistance increase due to the passage of a particle that either has finite DC resistance or is an insulator. Their approach assumes that the measurement takes place in an infinitely long channel, and neglects the inhomogeneity of the field due to a short aperture length.



Z_0 is the impedance of the solution-filled channel of complex conductivity s_1 and ϵ_1 . Z_1 is the impedance with a cell present. The equivalent frequency dependent conductivity $s^*(\omega)$ and permittivity $\epsilon^*(\omega)$ of the channel are given by inhomogeneous media dispersion theory and geometric capacitance or using FEM simulations. ΔZ is defined as the impedance difference between these two states $\Delta Z = Z_1 - Z_0$ taking into account the electrode polarization effect as well as stray impedances.

Dielectric spectroscopy:

In dielectric spectroscopy, the impedance of a biological suspension is measured using an ac excitation signal. The suspension is held in a measurement cell containing two, three or four electrodes. The current passing through the system is measured as a function of frequency to give the electrical properties of the particles in suspension. The development of techniques for single particle analysis using ac electrokinetic methods, primarily electrorotation and dielectrophoresis. AC electrokinetics is the study of the behaviour of particles (movement and/or rotation) subjected to an ac electric field. Electrical forces act on both the particles and the suspending fluid and have their origin in the charge and electric field distribution in the system

Microfluidic cytometry:

Flow cytometry is a technique in which the properties of large numbers of cells are measured at high speed, one cell at a time. The device measures the dc resistance between two electrically isolated fluid-filled chambers as cells pass through a small connecting orifice. For a fixed sized orifice, the change in electrical current can be used to count and size the cells. In the most general configuration, a number of individual ac signals are mixed and applied to the top microelectrodes each signal representing a single probe frequency that is applied continuously. The signals generate an electric field in the channel, and when a cell passes through the device the electric field is perturbed, causing a change in the current. This current change is measured in differential mode, using two closely positioned detection volumes defined by the one pairs of electrodes. As a cell passes through the electrode gap, this electrode sensing the current change. The change in electric current depends upon the size, shape and dielectric properties of the particle through the change in impedance of the detection area.

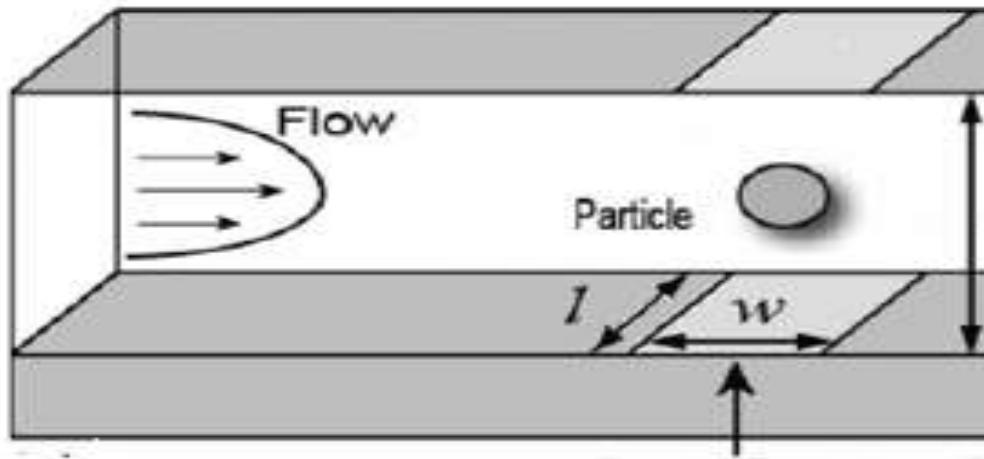
Sample preparation:

- Whole blood sample should be from a healthy adult by venipuncture.
- The blood sample obtained is to be pre-tested for communicable diseases.
- Then it should be mixed with anticoagulant (to prevent coagulation)
- Such as
 - EDTA solution
 - 3.8% buffered sodium citrate
- Then the blood is to be diluted with physiological saline solution (0.9 % NaCl) to prepare blood samples of desired hematocrit levels like 2 %, 5 %, 10 %, 20 % and 45 %.
- Considering the low shelf life of these blood samples, experiments were conducted within 5 days from the date of blood collection.

- Before starting the experiments, the chip was thoroughly flushed with saline solution
- Blood samples with different hematocrit levels (2 %, 5 %, 10 %, 20 %, 45 %) were then introduced at the inlet.
- To ensure uniform mixing of the blood, the beaker containing the source blood was stirred at frequent intervals

Cell counting:

- Number of cells in the blood samples and collected plasma is quantified by the cell counting method
- Now a constant current is set using a pair of electrodes and a voltage or current pulse is recorded as each cell passes through orifice

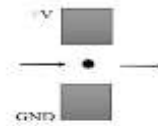


- As a cell passes through the electrode gap, the current changes.
- The change in electric current depends upon the size, shape and dielectric properties of the particle
- the resistance increase due to the passage of a particle that either has finite DC resistance or is an insulator

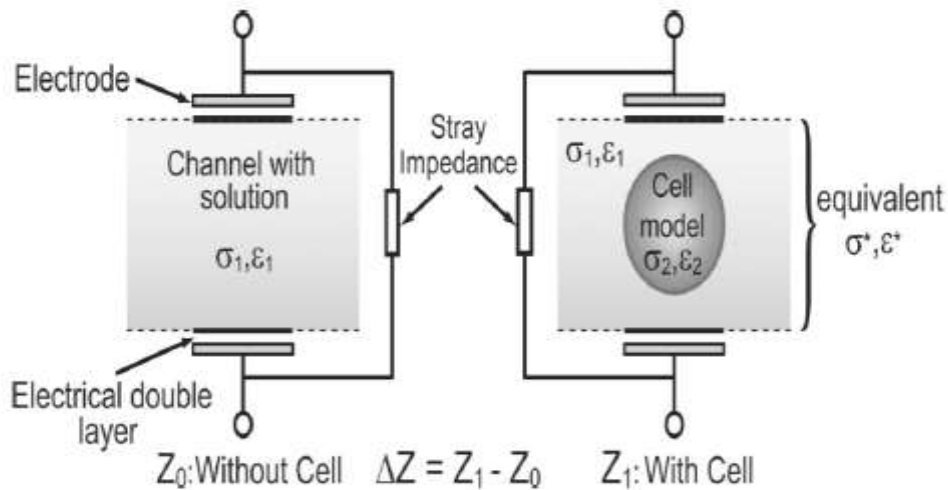


- By monitoring such pulses in electric current, the number of particles for a given volume of fluid can be counted.
- The two electrodes are connected through the liquid medium. An AC voltage is applied to the electrodes.
- Whenever there is a cell in between them there is a change of resistance in the circuit (ΔR).
- The change in resistance is represented by:

$$\Delta R = \frac{\rho}{A^2} v_p$$



- Where A is the cross sectional area of the channel, ρ is the specific resistance of the medium, v_p is the volume of the cell. A and ρ remains constant hence the magnitude of ΔR depends on v_p



Flow rate ratio (F_Q):

$$F_Q = \frac{Q_1}{Q_2} = \frac{L_p W_b \left\{ 1 - 0.63 \left(\frac{h_b}{W_b} \right) \right\}}{L_b W_p \left\{ 1 - 0.63 \left(\frac{h_p}{W_p} \right) \right\}}$$

- L_p and W_p are the length and width of plasma channel, respectively; L_b and W_b are the corresponding dimensions for the main blood channel.

Channel resistance:

$$R = \frac{12\mu L}{\left\{1 - 0.63\left(\frac{h}{w}\right)\right\} h^3}$$

- L , h and w were the length, depth and width of the microchannel, respectively and μ is the viscosity of blood sample

• **Separation efficiency :**

$$\eta = \frac{c_s - c_p}{c_s} * 100$$

- c_s = Number of cells per μl in source/feed blood at inlet of microchannel
- c_p = Number of cells per μl in depleted cell branch or plasma collection outlet of the microchannel

The Reynolds number : (at the inlet)

$$R_e = \frac{\rho v d_h}{\mu}$$

- $d_h = \frac{4 * \text{Area of microchannel}}{\text{Perimeter of microchannel}}$
- $v = \frac{\text{Total Flow rate}}{\text{area of the microchannel}}$
- d_h is the hydraulic diameter
- v is the average velocity
- ρ = density of blood
- μ = viscosity of blood.

References

- [1]. Siddhartha Tripathi & Amit Prabhakar & Nishant Kumar & Shiv Govind Singh & Amit Agrawal 25 January 2013 . Springer Science+Business Media New York.
“Blood plasma separation in elevated dimension T-shaped microchannel”
- [2]. Shady Gawad,* Karen Cheung, Urban Seger, Arnaud Bertsch and Philippe Renaud LMIS-IMM-STI, EPFL, 1015 Lausanne, Switzerland.October 2003, accepted 22nd December 2003 ”Dielectric spectroscopy in a micromachined flow cytometer”.
- [3]. Hywel Morgan, Tao Sun, David Holmes, Shady Gawad¹ and Nicolas G Green. Nanoscale Systems Integration Group, School of Electronics and Computer Science, University of Southampton, SO17 1BJ UK 15 December 2006.
“Single cell dielectric spectroscopy”
- [4]. Bond Strength Characterization of SU-8 to SU-8 for Fabricating Microchannels of an Electrokinetic Microfluidic Pump 2012 Nash Anderson. Materials Engineering Department
- [5]. Harvard-MIT Division of Health Sciences and Technology HST.410J: Projects in Microscale Engineering for the Life Sciences, Spring 2007 Course Directors: Prof. Dennis Freeman, Prof. Martha Gray, and Prof. Alexander Aranyosi
Manufacturing a PDMS microfluidic device via a Silicon Wafer Master Eric Lam, Tri Ngo
- [6]. Santeri Tuomikoski¹ and Sami Franssila Microelectronics Centre, Helsinki University of Technology, PO BOX 3500, 02015 TKK, Finland Received August 22, 2003; accepted September 23, 2003 “Wafer-Level Bonding of MEMS Structures with SU-8 Epoxy Photoresist”

- [7]. CEPSR Clean Room at Columbia University - SU-8 Photoresist Process
- [8]. Hao-Yu Greg Lin, (617) 384-5028, -CNS STANDARD OPERATING PROCEDURE SOP084 SU-8 Process Training
- [9]. PROTOCOL FOR PHOTOLITHOGRAPHY USING MYLAR MASKS (IN BNC) Debkishore Mitra March, 2009
- [10]. SU-8 2000 Permanent Epoxy Negative Photoresist PROCESSING GUIDELINES FOR: SU-8 2025, SU-8 2035, SU-8 2050 and SU-8 2075
- [11]. Harvard-MIT Division of Health Sciences and Technology HST.410J: Projects in Microscale Engineering for the Life Sciences, Spring 2007 Course Directors: Prof. Dennis Freeman, Prof. Martha Gray, and Prof. Alexander Aranyosi
- [12]. Manufacturing a PDMS microfluidic device via a Silicon Wafer Master *SU-8 Photolithography and Its Impact on Microfluidics* Rodrigo Martinez-Duarte and Marc J.
- [13]. Continuous flow separations in microfluidic devices Nicole Pamme Received 20th August 2007, Accepted 2nd October 2007 First published as an Advance Article on the web 2nd November 2007 DOI: 10.1039/b712784g